Citation: Cell Death and Disease (2012) 3, e418; doi:10.1038/cddis.2012.159

www.nature.com/cddis

Autophagy as a new therapeutic target in Duchenne muscular dystrophy

This article has been corrected since Online Publication and a corrigendum has also been published

C De Palma[1], F Morisi[2,8], S Cheli[1,8], S Pambianco[1], V Cappello[3,4], M Vezzoli[5], P Rovere-Querini[5], M Moggio[6], M Ripolone[6], M Francolini[3], M Sandri*[,7] and E Clementi*[,1,2]

A resolutive therapy for Duchene muscular dystrophy, a severe degenerative disease of the skeletal muscle, is still lacking. Because autophagy has been shown to be crucial in clearing dysfunctional organelles and in preventing tissue damage, we investigated its pathogenic role and its suitability as a target for new therapeutic interventions in Duchenne muscular dystrophy (DMD). Here we demonstrate that autophagy is severely impaired in muscles from patients affected by DMD and *mdx* mice, a model of the disease, with accumulation of damaged organelles. The defect in autophagy was accompanied by persistent activation via phosphorylation of Akt, mammalian target of rapamycin (mTOR) and of the autophagy-inhibiting pathways dependent on them, including the translation-initiation factor 4E-binding protein 1 and the ribosomal protein S6, and downregulation of the autophagy-inducing genes *LC3*, *Atg12*, *Gabarapl1* and *Bnip3*. The defective autophagy was rescued in *mdx* mice by long-term exposure to a low-protein diet. The treatment led to normalisation of Akt and mTOR signalling; it also reduced significantly muscle inflammation, fibrosis and myofibre damage, leading to recovery of muscle function. This study highlights novel pathogenic aspects of DMD and suggests autophagy as a new effective therapeutic target. The treatment we propose can be safely applied and immediately tested for efficacy in humans.

Cell Death and Disease (2012) **3,** e418; doi:10.1038/cddis.2012.159; published online 15 November 2012
Subject Category: Experimental Medicine

Muscular dystrophies are a group of genetic, hereditary muscle diseases characterised by defects in muscle proteins. These defects result in progressive skeletal muscle damage accompanied by myofibre necrosis and chronic local inflammation, leading to substitution of myofibres by connective and adipose tissue.[1] In Duchenne muscular dystrophy (DMD), the most severe form of these diseases, the continuous and progressive skeletal muscle damage leads to complete paralysis and death of patients, usually by respiratory and/or cardiac failure.[2]

The therapeutic protocols currently in use, based on corticosteroid administration, provide some delay in the progression of the disease, but they are associated with severe side effects.[3,4] Therapies that substitute corticosteroids or at least may act as corticosteroid-sparing drugs are thus being actively pursued, and biological mechanisms relevant to skeletal muscle homoeostasis are explored, in order to identify new targets.

Autophagy is emerging as an important process that limits muscle damage.[5,6] Inhibition/alteration of autophagy contributes to myofibre degeneration leading to accumulation of abnormal organelles.[7,8] Mutations that inactivate Jumpy, a phosphatase that counteracts the activation of VPS34 for autophagosome formation and reduces autophagy, are associated with a centronuclear myopathy.[9] This observation suggests that unbalanced autophagy is pathogenic in muscle degeneration. Likewise, hyperactivation of Akt as a consequence of muscle-specific deletion of the mammalian target of rapamycin (mTOR) leads to inhibition of autophagy and to a muscle phenotype resembling the one observed in muscular dystrophy.[10]

The validity of autophagy modulation as a therapeutic strategy has been shown in a mouse model of Ulrich

[1]Unit of Clinical Pharmacology, Department of Biomedical and Clinical Sciences, University Hospital L. Sacco, Università di Milano, Milan, Italy; [2]E.Medea Scientific Institute, Bosisio Parini, Lecco, Italy; [3]Department of Medical Biotechnology and Translational Medicine, Consiglio Nazionale delle Ricerche Institute of Neuroscience, Università di Milano, Milan, Italy; [4]CNI@NEST Istituto Italiano di Tecnologia, Pisa, Italy; [5]Innate Immunity and Tissue Remodelling Unit, Division of Regenerative Medicine, Stem Cells and Gene Therapy, Milan, Italy; [6]Neuromuscular Unit, Fondazione IRCCS Ca' Granda Ospedale Maggiore Policlinico, Milano, Dino Ferrari Centre, Università di Milano, Milan, Italy and [7]Department of Biomedical Science, University of Padova, Dulbecco Telethon Institute at Venetian Institute of Molecular Medicine, Padova, Italy

*Corresponding authors: M Sandri, Department of Biology, Venetian Institute of Molecular Medicine, University of Padova, Padova, Italy. Tel: +39 049 7923 258; Fax: +39 049 7923 250; E-mail: marco.sandri@unipd.it

or E Clementi, Unit of Clinical Pharmacology, Department of Biomedical and Clinical Sciences, University Hospital L. Sacco, Università di Milano, Via GB. Grassi 74, Milano 20157, Italy. Tel: +39 025 0319 683; Fax: +39 025 0319 646; E-mail: emilio.clementi@unimi.it

[8]These authors contributed equally to this work.

Keywords: autophagy; Duchenne muscular dystrophy; therapy

Abbreviation: DAPI, 4′,6-diamidino-2-phenylindole; DMD, Duchenne muscular dystrophy; mTOR, mammalian target of rapamycin; WT, wild-type; TA, tibialis anterior; LC3, microtubule-associated protein-1 light chain 3; 4E-BP1, eukaryotic translation-initiation factor 4E-binding protein 1; SD, standard diet; LPD, low-protein diet; CSA, cross-sectional area; TUNEL, TdT-mediated dUTP-biotin nick end labelling; EBD, Evans blue dye; H&E, haematoxylin and eosin.

Received 25.7.12; revised 07.9.12; accepted 25.9.12; Edited by G Melino

myopathy characterised by defective autophagy and accumulation of dysfunctional organelles.[11,12] Forced reactivation of autophagy in these animals yielded a beneficial therapeutic response.[11]

Indirect evidence indicates a possible role of deficient autophagy also in DMD pathogenesis. Higher levels of activation and phosphorylation of Akt are observed in muscles and primary myoblasts of the *mdx* mouse model of dystrophy.[13,14] In agreement with this observation, the progressive muscular dystrophic phenotype observed in *mdx* mice is accompanied by progressively enhanced Akt activation especially at peak necrotic and hypertrophic phases of disease.[14] Such a phenotype has also been described in patients affected by DMD.[14] Akt is the most potent inhibitor of autophagy in skeletal muscle, blocking formation of autophagosomes and lysosomal-dependent degradation of their content,[15,16] thereby suggesting a defective autophagic process. Moreover, histo-pathological hallmarks of DMD, namely protein aggregation, presence of swollen and damaged mitochondria, as well as distension of sarcoplasmic reticulum, are often observed when autophagy is impaired.[17,18]

The molecular pathways and the role of autophagy in DMD had not yet been investigated. We have now investigated the autophagic machinery in the *mdx* mouse model of DMD and in muscle tissues from DMD-affected patients. We found by *in vivo* and *ex vivo* analyses that autophagy is defective in both the human and mouse muscular dystrophy and that such defect contributes to the pathogenesis of the disease. Furthermore, we show that pharmacological reactivation of autophagy restores muscle structure and function. Our results identify autophagy as an important homoeostatic mechanism deranged in dystrophic muscles and indicate that novel therapeutic approaches aimed at reactivating autophagy are a valuable strategy to reduce muscle damage in DMD.

Results

Autophagy is reduced in *mdx* mice. To explore the status of autophagy in the dystrophic muscle, we compared key markers of autophagy in muscles from 4-month-old *mdx* and wild-type (WT) mice. We examined tibialis anterior (TA) and diaphragm muscles, because they are good examples of muscles relying on glycolytic and oxidative metabolism,[11] respectively, and closely mimic typical features of human muscular dystrophy, including myofibres with central nuclei and clustering of inflammatory cells.[13]

As shown in Figure 1a, the levels of the lipidated form of the microtubule-associated protein-1 light chain 3 (LC3 II), which is generated during autophagosome formation and reflects active autophagy,[19] were significantly lower in muscles from *mdx* than in those of WT animals. The levels of p62, a protein known to be incorporated into autophagosomes and efficiently degraded,[20] were instead increased.

We found enhanced levels of Akt in both TA and diaphragm muscles from *mdx* mice as already described.[13,14] Of importance, we also found that phosphorylation of Akt on Ser473 was significantly increased as it was the phosphorylation of key downstream effectors of mTOR, namely the ribosomal protein S6 and the eukaryotic translation-initiation factor 4E-binding protein 1 (4E-BP1) (Figure 1b). Phosphorylation of these proteins leads to their activation, which in muscle may lead to inhibition of autophagy.[21]

Akt phosphorylation maintains mTOR in its active form and prevents FoxO3 translocation from the cytoplasm to the nucleus with ensuing transcriptional inhibition of genes essential to autophagosome formation.[12] In agreement with this, we found lower mRNA expression of autophagy-related genes directly regulated by FoxO3, that is, *LC3*, *Atg12*, *Gabarapl1* and *Bnip3* in *mdx* mouse muscles (Figure 3e), indicating that FoxO3 downstream targets are impaired in

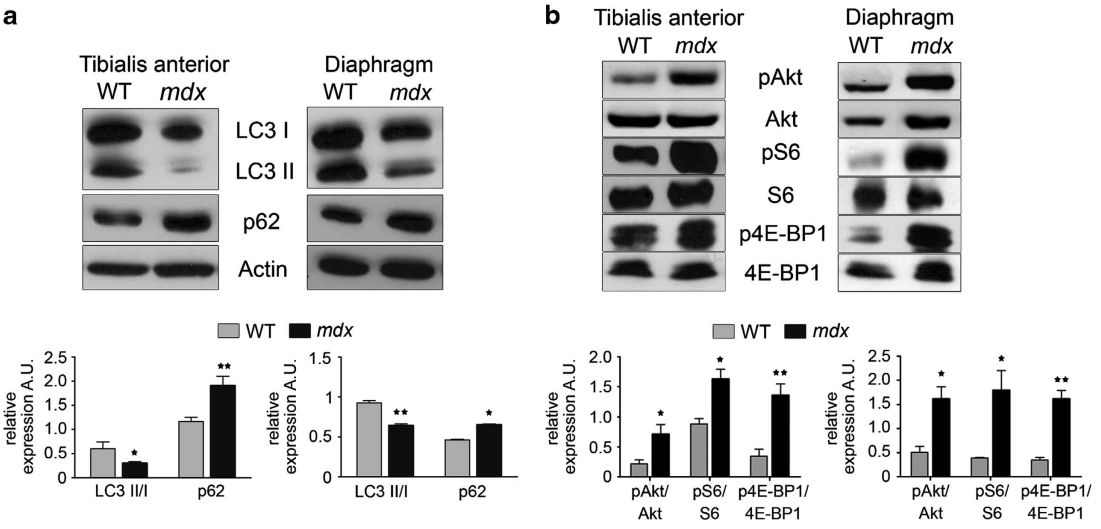

Figure 1 Autophagy is defective in *mdx* mice. (**a**) Muscle homogenates from *mdx* and WT mice (60 μg per lane) were immunoblotted with antibodies against LC3 and p62. LC3 lipidation (LC3 II) in TA and in diaphragm muscles of *mdx* mice is reduced when compared with that of WT mice. The *mdx* mice also show accumulation of p62. Densitometric quantification of the LC3 II/I ratio and of p62, normalised against actin, is also shown. (**b**) In muscle homogenates (60 μg per lane), phosphorylation levels of Akt, S6 and 4E-BP1 are enhanced in *mdx* mice when compared with those of WT. We used the same protein extracts as in panel **a**. Densitometric analyses show the ratio between phosphorylated and corresponding total protein. In both panels, western blots are representative, and quantifications correspond to 15 animals per group. The asterisks indicate statistical significance *versus* WT (*$P<0.05$ and **$P<0.01$). Error bars represent S.E.M.

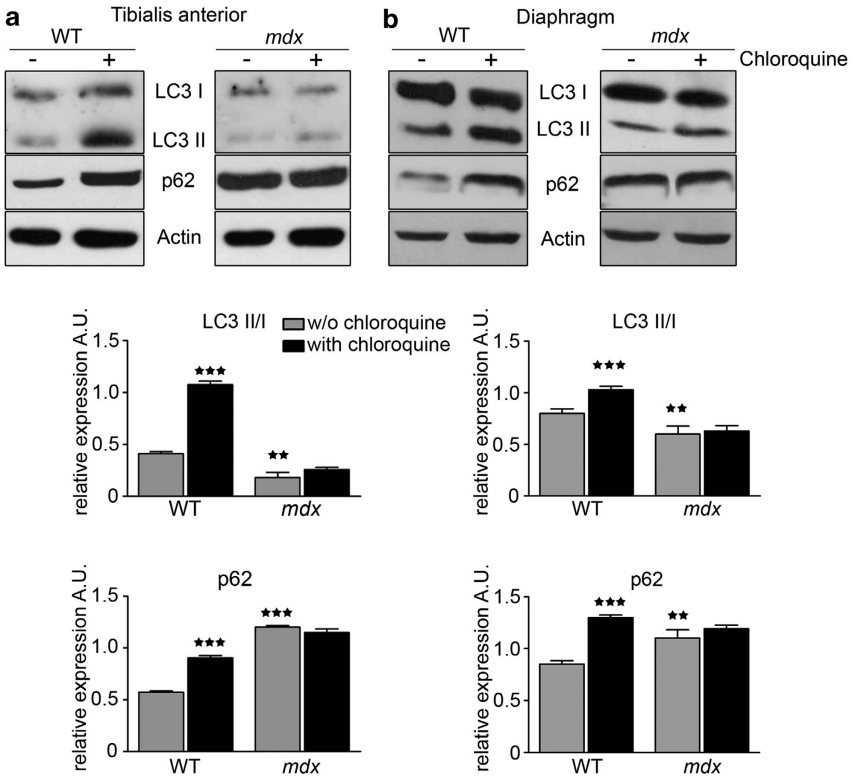

Figure 2 Chloroquine treatment of WT and *mdx* mice. (**a** and **b**) The western blots show the levels of LC3 and p62 in TA (**a**) and diaphragm (**b**) muscles of *mdx* and WT mice treated (+) or not (−) with chloroquine diphosphate at 50 mg/kg body weigh daily for 7 days. The absence of choloroquine effects in *mdx* (but not WT) mice indicate that the defect in LC3 II expression is due to an actual deficit of autophagy and not the consequence of autophagic vesicle exhaustion secondary to hyperactivation of autophagy. Western blotting are representative, and quantifications correspond to 15 animals per group. Asterisks indicate statistical significance *versus* untreated WT (**$P<0.01$ and ***$P<0.001$). Error bars represent S.E.M.

mdx mice and providing a molecular correlate to the observed deficiency in autophagy.

Reduced autophagy in *mdx* mice is due to defective pro-autophagic signalling. Reduced LC3 II levels may depend on direct inhibition of autophagic flux; alternatively, they may be due to progressive exhaustion of LC3 II-containing vesicles following a hyperactivation of autophagy. To discriminate between these two possibilities, we used chloroquine, a lysosomal inhibitor that blocks the degradation of autophagosomes and their content, including of LC3 and p62.[22] Mice were treated with chloroquine, administered at the dose of 50 mg/kg body weight per day, for 7 days. This treatment led to significant increases in the levels of LC3 bands and p62 in both TA and diaphragm muscles of WT animals; such increases were not observed in the corresponding samples of *mdx* mice (Figures 2a and b). These data indicate that the reduced LC3 II levels observed in *mdx* mouse muscles are not the consequence of vesicles exhaustion secondary to a hyperactive autophagic process.

We next subjected mice to short-term starvation (6 and 15 h of fasting), a treatment that activates autophagic signalling in different organs, including in muscles.[23] Starvation enhanced LC3 II levels with increased LC3 II/I ratio in TA and diaphragm muscles of WT mice; the levels of p62 were instead reduced, consistent with its enhanced degradation (Figures 3a and b and Supplementary Figure S1a). No effects of starvation on LC3 II and p62 levels were instead observed in *mdx* mouse muscles (Figures 3a and b and Supplementary Figure S1a). Chloroquine enhanced the LC3 II/I ratio further and induced accumulation of p62 in muscles from WT animals, whereas it was completely ineffective in *mdx* mouse muscles (Figures 3a and b).

In agreement with these results, starvation decreased significantly phospho-Akt and phospho-4E-BP1 levels in WT animals (Figures 3c and d and Supplementary Figure S1b), where it also upregulated *LC3B, Atg12, Bnip3* and *Gabarapl1* mRNA levels (Figure 3e), consistent with Akt and mTOR signalling inhibition and with autophagy induction.

No changes in protein phosphorylation or mRNA expression were instead observed in *mdx* mouse muscles after starvation, indicating a deficiency in pro-autophagic signalling (Figures 3c and e).

We then analysed the ultrastructure of TA of WT and *mdx* mice in basal conditions (Figures 4a and c). We detected defects neither in the architecture of the contractile apparatus nor in the mitochondrial pool of WT muscles (Figure 4a and inset); in *mdx* mice, although the contractile apparatus seemed mostly unaffected (Figure 4c), we observed an expansion of the *cisternae* of the endoplasmic reticulum in subsarcolemmal regions, where they occasionally form swollen stacks (Supplementary Figures S2a and b); this feature was even more prominent in starved *mdx* mice (Figure 4d). Moreover, in tissues from *mdx* mice, infiltrating

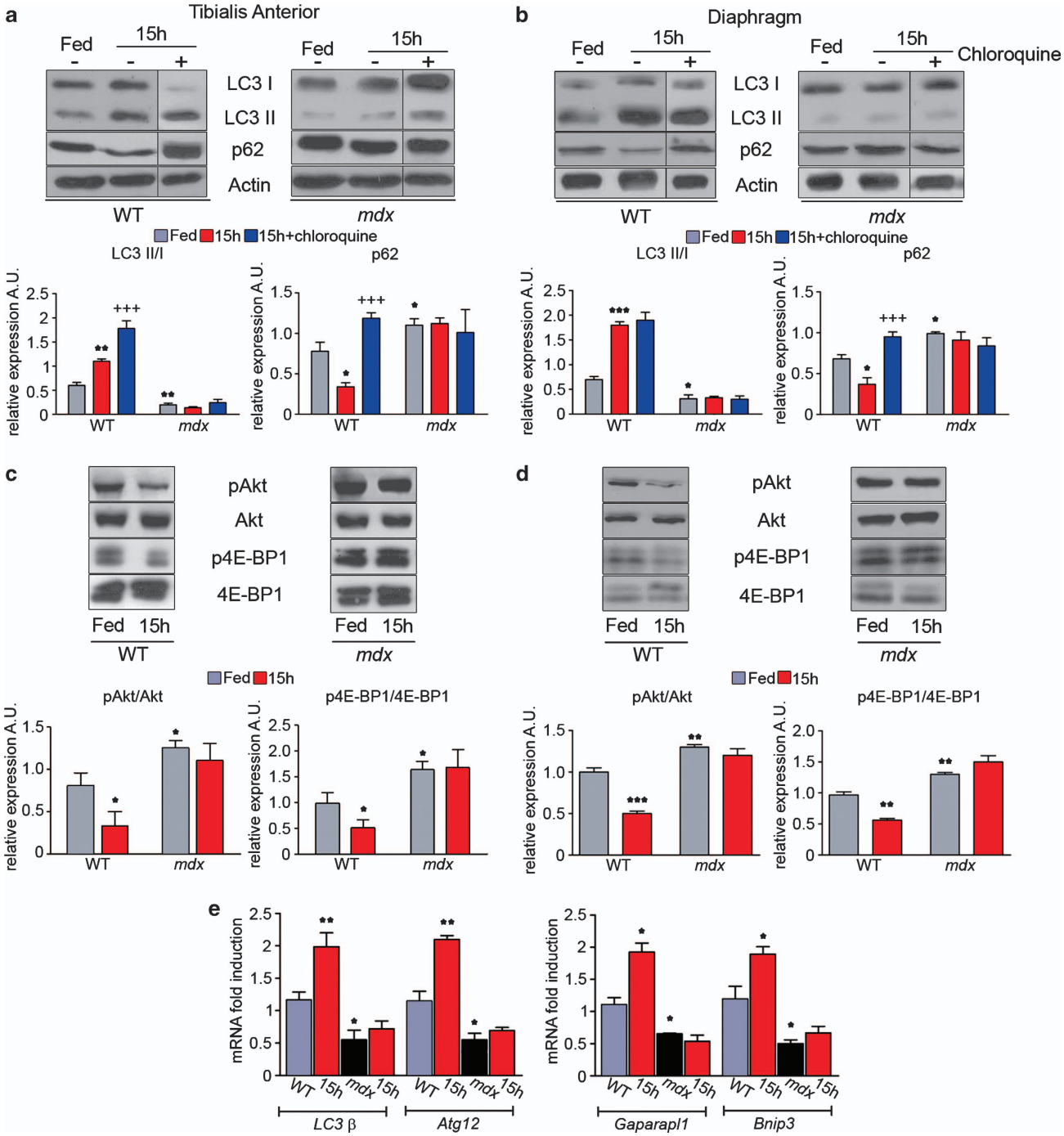

Figure 3 Autophagy induction is impaired in *mdx* mice. (**a** and **b**) Western blots showing LC3 and p62 levels in TA (**a**) and diaphragm (**b**) muscles (60 μg per lane) of fed and 15 h-starved (15 h) WT and *mdx* mice, treated (+) or not (−) with chloroquine 50 mg/kg body weight daily for 7 days. Densitometric quantification of LC3 II/I ratio and of p62 levels, normalised against actin, shows induction of autophagy only in WT mice after 15 h of starvation. (**c** and **d**) Western blots, using the same protein extracts of panels **a** and **b**, reveal reduction of Akt and 4E-BP1 phosphorylation in diaphragm and TA muscles of 15 h-starved WT mice. The *mdx* muscles display no changes in the phosphorylation levels of both proteins. (**e**) Quantitative RT-PCR analysis of *LC3β*, *Atg12*, *Gaparapl1* and *Bnip3* mRNA levels in diaphragm and TA muscles of fed and 15 h-starved WT and *mdx* mice. The genes downstream of FoxO3 are upregulated in WT mice after starvation, but not in the *mdx* mice. Western blots are representative, and quantifications correspond to 15 animals per group. Asterisks indicate statistical significance *versus* WT-fed mice (*$P<0.05$, **$P<0.01$ and ***$P<0.001$); crosses indicate statistical significance *versus* WT-starved mice ($^{+++}P<0.001$). Error bars represent S.E.M.

cells and collagen fibres were seen among myofibres (Supplementary Figures S2c and d). In muscles derived from WT-starved animals (Figure 4b), we observed the presence of autophagosomes associated with intracellular organelles (mostly mitochondria, Figure 4b inset); in contrast, in muscles derived from starved *mdx* mice, although damaged organelles were observed (mainly mitochondria of the subsarcolemmal pool), these were never associated with autophagosomes (Figure 4d).

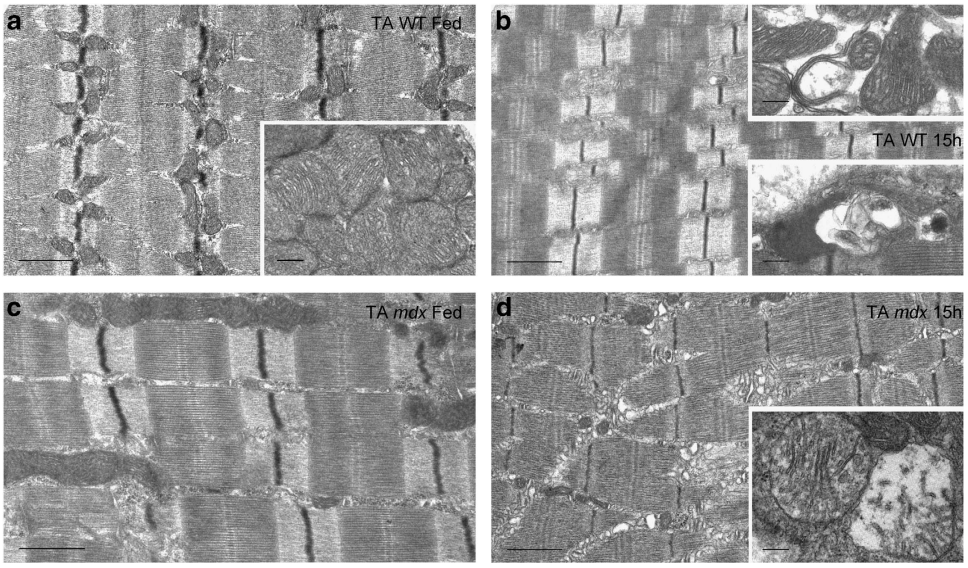

Figure 4 Autophagy induction in WT and *mdx* mice. (**a**) electron micrographs of TA muscles from WT mice. No defects in the architecture of the contractile apparatus or in the mitochondrial pool are observed in WT-fed mice (scale bars 1 μm, 200 nm in the inset). (**b**) The 15 h-starved TA muscles of WT mice (**b** and insets) show alteration of mitochondrial pool and an increase of autophagosomes, identified as double-membrane structures associated with degenerating organelles (inset) (scale bars 1 μm, 200 nm in the insets). **(c)** Electron micrographs of TA muscles from fed *mdx* mice. No autophagosomes are detectable, and the defect in autophagy is accompanied by expansion of endoplasmic reticulum *cisternae* expansion (scale bar 1 μm). (**d**) The *mdx*-starved TA muscles present an increased level of altered organelles, in particular of mitochondria in the subsarcolemmal pool, that are not related with lytic organelles (**d** and inset) (scale bars 1 μm, 200 nm in the inset). Images are representative of reproducible results in 10 animals per group

Autophagy reactivation improves the dystrophic phenotype of *mdx* mice. A specific dietary regimen, characterised by low amino-acid intake, but with the same caloric value of standard food was shown to ameliorate the dystrophic feature of *Col6*$^{-/-}$ mice by enhancing in a chronic and physiological manner skeletal muscle autophagic machinery.[11,12] We investigated whether a 3-month treatment with such a low-protein diet (LPD) reactivated autophagy in *mdx* mice and the impact of this effect on the dystrophic phenotype. LPD treatment enhanced expression of LC3 II and reduced that of p62 in TA and diaphragm not only in WT but also in *mdx* mice, with dephosphorylation, and thus inactivation, of Akt and 4E-BP1 (Figures 5a and b). Consistently, we observed enhanced RNA levels of authopagic genes downstream to FoxO3 (Figure 5c and data not shown). Such an effect was not observed in mice treated with a control, standard diet (SD). Thus a long-term LPD was able to reactivate autophagy in *mdx* mice.

We then investigated the therapeutic efficacy of the LPD treatment. In LPD-treated *mdx* mice, the Whole Body Tension measurement, which determines the total phasic forward pulling tension exerted by the fore and hind limb muscles,[24,25] was significantly improved as compared with SD-treated animals (Figure 5c). Histological analyses by the haematoxylin and eosin (H&E) staining revealed a degenerated muscle status in SD-treated *mdx* mice; in contrast, muscle architecture was nearly normal in LPD-treated mice, with a significantly lower number of necrotic myofibres (Figure 5d). The beneficial effect of the diet was also apparent when the myofibre cross-sectional area (CSA) was investigated. The heterogeneity in myofibre CSA observed in SD-treated *mdx* mice, in which values ranged between 250 and 3000 μm^2, with the largest diameters being a sign of degeneration (pathological hypertrophy) (Figure 5e), was normalised in LPD-treated animals, with significantly more homogeneous frequency histograms and CSA values not significantly different from those observed in WT animals.

The percentage of apoptotic nuclei, measured using the TdT-mediated dUTP-biotin nick end labelling (TUNEL) method, was significantly lower in LPD-treated compared with SD-treated *mdx* mice, both in TA and diaphragm (Figure 6c). This finding suggests that the treatment with LPD reduced also the programmed death of myofibres. Interestingly, LPD treatment in *mdx* mice increased also the number of centronucleated myofibres (Figure 5d), indicating a benefit on muscle regeneration. Consistently, fibrosis and collagen accumulation was reduced in LPD-treated animals as assessed by the Masson's Trichrome staining (Figure 6a).

Muscles of LPD-treated *mdx* mice showed an uptake of the Evans blue dye (EBD) injected i.v., which was significantly reduced with respect to that in SD-treated mice (Figure 6b). Because EBD stains damaged myofibres,[26] this finding indicates that the treatment reduced the fragility of sarcolemmas in *mdx* mice.[26]

It is noteworthy that long-lasting induction of autophagy in WT led to minor muscle alterations, as previously demonstrated by others,[11] including the increase of apoptotic degeneration of the myofibres, shown by an increased number of TUNEL-positive nuclei (Figure 6c). This was expected because previous studies have already demonstrated that excessive autophagy induction is detrimental for muscle homoeostasis in healthy conditions, further highlighting the importance of a balanced autophagic flux.

Autophagy is defective in human DMD patients. We assessed whether the defect in autophagy observed in *mdx*

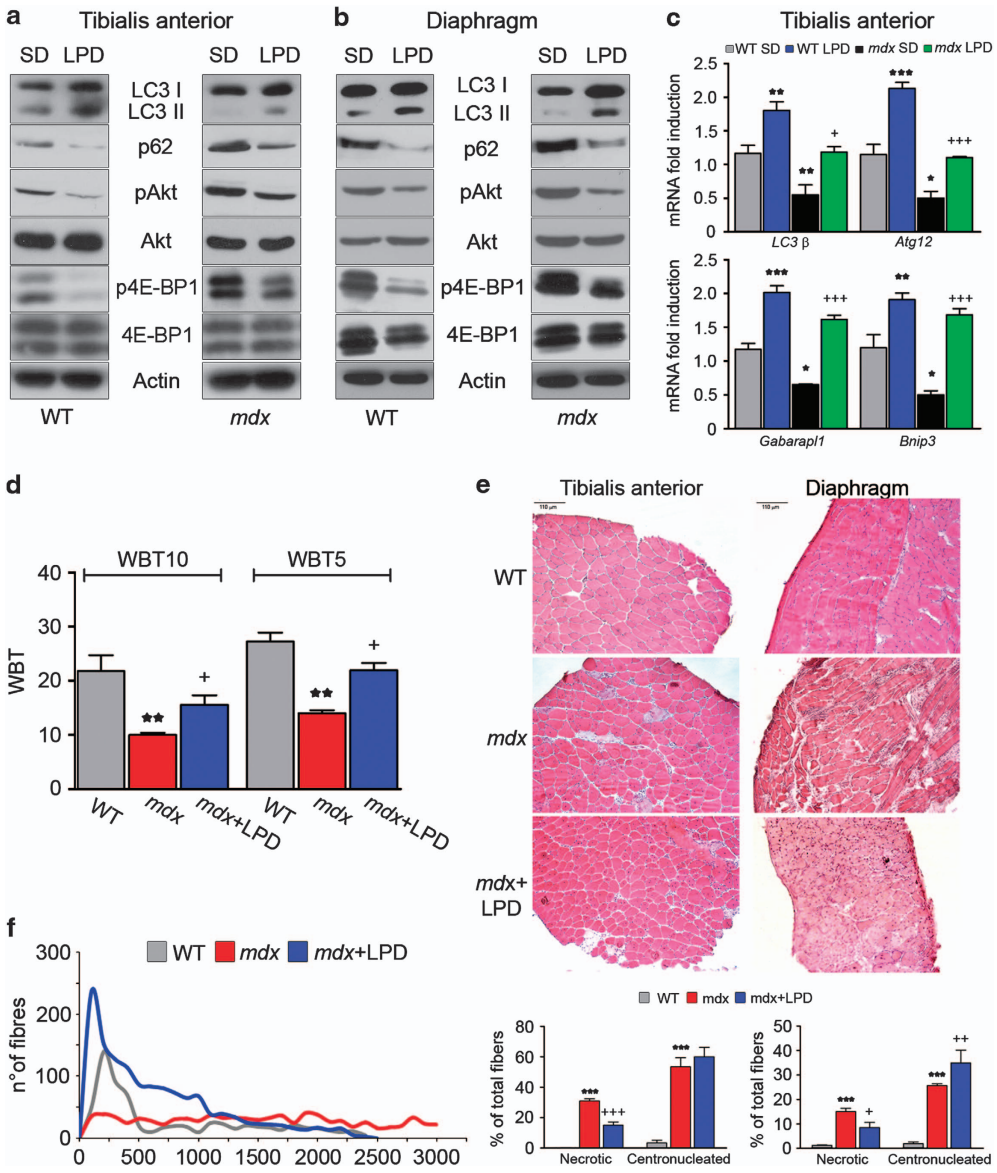

Figure 5 Prolonged autophagy induction by LPD ameliorates dystrophy in *mdx* mice. WT and mdx mice were fed with LPD or SD for 3 months. (**a** and **b**) The representative western blots of homogenates (60 μg per lane) from TA (**a**) and diaphragm (**b**) muscles show that LPD enhances LC3 II and p62 expression, whereas reducing phosphorylation of Akt and 4E-BP1 both in WT and *mdx* mice. **(c)** Quantitative RT-PCR analysis of *LC3β*, *Atg12*, *Gaparapl1* and *Bnip3* mRNA levels in TA fed with SD or LPD. (**d**) *In vivo* analysis of muscle force was measured as the amount of whole body pulling force, calculated as the force relative to body weight in WT and *mdx*. WBT10 represents the media of 10 FPTs, measured as grams of tension, divided by body weight. WBT5 represents the media of top-five FPTs divided by body weight. LPD improved muscle force in *mdx* mice. (**e**) TA and diaphragm muscles were stained with H&E; centronucleated and necrotic myofibres were counted. LPD reduces necrotic myofibres and increases centronucleated myofibres. Scale bar 110 μm. (**f**) Distribution of CSA values of 700 myofibres of TA muscle of WT and *mdx* treated with LPD or SD. LPD normalises the CSA distribution in *mdx*. Images and western blots in the various panels are representative, and quantifications correspond to 15 animals per group. Asterisks indicate statistical significance *versus* WT (*$P<0.05$, **$P<0.01$ and ***$P<0.001$); crosses indicate statistical significance *versus mdx* normally fed ($^{+}P<0.05$; $^{++}P<0.01$ and $^{+++}P<0.001$). Error bars represent S.E.M.

mice applied also to the human disease. We analysed muscle biopsies from five DMD-affected patients and four relative controls. All tissues from DMD patients showed significantly lower levels of LC3 II and significant accumulation of p62 with respect to tissues from the controls (Figure 7a). In addition, they showed enhanced phosphorylation of Akt and of 4E-BP1 (Figure 7b), indicating that the pathway affected in DMD patients is identical to the one observed in *mdx* mice leading to a multi step inhibition of autophagy.

Discussion

In this study, we report that autophagy is defective in DMD, that defects in autophagy contribute significantly to the pathology of DMD, and that pharmacological strategies that reactivate autophagy have beneficial effects that can be exploited in therapeutic perspective. Moreover, we characterise the signalling mechanisms involved in autophagic deficiency in DMD.

The defect in autophagy was demonstrated by biochemical and ultrastructural analyses. We found a significant reduction

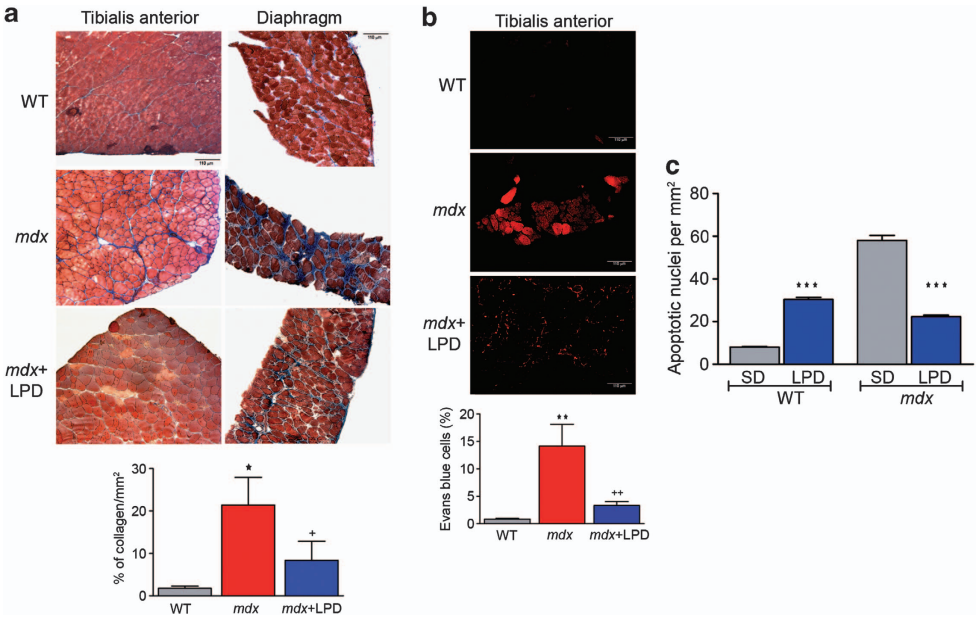

Figure 6 Prolonged autophagy induction by LPD ameliorates dystrophy in *mdx* mice. WT and mdx mice were fed with LPD or SD for 3 months. (**a**) TA and diaphragm muscles representative sections, stained with the Masson's Trichrome procedure reveal reduced accumulation of collagen and fibrosis in LPD-treated *mdx versus* SD-treated *mdx*. Scale bar 110 μm. The graph shows the quantification carried out in five sections per animal. (**b**) Fibre membrane damage, evaluated by assessing EBD uptake, quantified by the Image 1.63 (Scion Corporation) software as % of Evans blue-positive cells. The representative images show that LPD reduce EBD uptake in *mdx* mice. Scale bar 110 μm. The graph shows the quantification carried out in five sections per animal. (**c**) Quantification of TUNEL-positive nuclei in TA muscles of WT and *mdx* mice; LPD reduces the number of TUNEL-positive nuclei compared with *mdx*. Quantification (number of TUNEL-positive nuclei normalised per mm^2) was carried out with the Image 1.63 (Scion Corporation) software. Images in the various panels are representative, and quantifications correspond to 10 animals per group. Asterisks indicate statistical significance *versus* WT (*$P<0.05$, **$P<0.01$ and ***$P<0.001$). Error bars represent S.E.M.

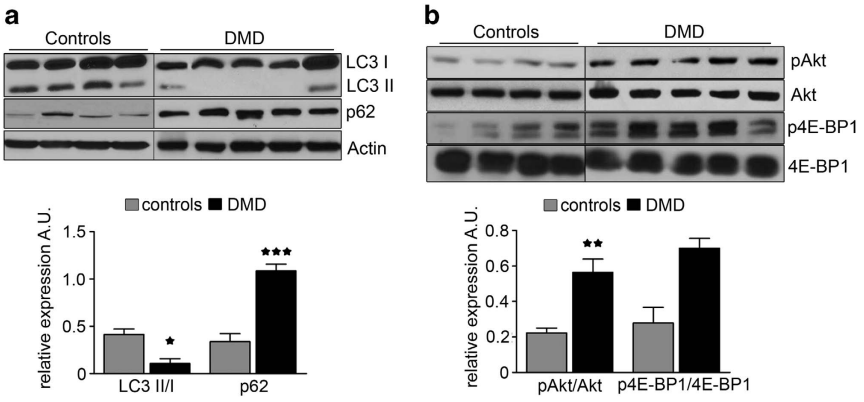

Figure 7 Autophagy is defective in human DMD patients. (**a**) Analysis of the LC3 ratio and p62 levels in human muscle biopsies from four control subjects and five DMD patients. p62 expression is normalised on GAPDH. (**b**) Western blots for pAKT and p4E-BP1 in protein lysates of human biopsies using the same protein extract of panel **a**. DMD patients show higher Akt and 4E-BP1 phosphorylation compared with controls. Western blots are representative, and quantifications correspond to results in biopsies from five DMD patients and four controls. Asterisks indicate statistical significance *versus* controls (*$P<0.05$ and **$P<0.01$). Error bars represent S.E.M.

in LC3 II, the active, lipidated form of LC3, in muscles from both DMD patients and *mdx* mice. The reduction in LC3 II was accompanied by clear signs of impaired autophagy at the ultrastructural level, with enhanced presence of damaged organelles. The reduction in the autophagic flux was further confirmed by the increase in p62 levels. The impairment in autophagy in the mouse model could not be rescued by up to 15 h of fasting, a treatment known to stimulate autophagic signalling in other conditions.[23] Restoration of autophagy, leading to increased levels of LC3 II and reduced levels of p62, required instead a long-term (3 months) treatment with a potent autophagy-reactivating treatment (LPD). These findings suggest that the defect in autophagy is due to an overall deficiency in the autophagic machinery rather than to a simple inhibition of the signalling pathways that stimulate autophagy.

When we investigated the autophagic signalling pathways and their alteration in muscular dystrophy, we found that inhibition of autophagy depended on Akt activation, as shown by its persistent phosphorylation reversible upon autophagy reactivation. Although we cannot exclude the intervention of multiple mechanisms, such as lysosomal defects, we found that downstream of Akt both the mTOR and FoxO3 pathways

were involved as shown by the persistent phosphorylation of 4E-BP1, and the downregulation of *Atg12*, *Bnip3* and *Gabarapl1* also reversed when autophagy was reactivated.

Although the role of FoxO3 signalling in autophagy in skeletal muscle has already been assessed and investigated fully,[15,16] our observation of a significant involvement of mTOR signalling in autophagy is an unexpected finding. To date, the role of mTOR in muscle autophagy, investigated in conditions different from DMD, that is, muscle atrophy and fasting conditions, was reported to be minor.[15,16,27] Indeed, inhibition of mTOR by rapamycin or its downregulation by RNA-mediated silencing in those settings was insufficient to induce autophagosome formation[15,16,27] and only slightly increased protein breakdown.[16] The observation of a relevant role of mTOR in *mdx* mice suggests that autophagy in DMD has characteristics and molecular constrains unique with respect to autophagy in other pathophysiological condition of skeletal muscle. A possible explanation of this specificity resides in the specific features of DMD, and the role of mTOR in it. Dystrophic muscle is characterised by repeated cycles of degeneration/regeneration, with the presence of regenerating and hypertrophic fibres generated as a compensatory mechanism due at least in part to hyperactivation of Akt and mTOR.[13,14] Although important, this functional compensation also leads to inhibition of autophagy.

The role of autophagy in DMD pathophysiology and its relevance as a therapeutic target was investigated in a long-term treatment of *mdx* mice with LPD. We evaluated carefully several unrelated markers of muscle function, damage and regeneration, and inflammatory responses. These markers were investigated using multiple different approaches in *mdx* mice after 3 months of treatment with the low protein or SDs. Our results clearly show that LPD treatment has therapeutic efficacy and ameliorates the dystrophic phenotype of *mdx* mice. Indeed, we observed a significant recovery of muscle function, as shown by the improvement of whole body tension, accompanied by reduced muscle fibrosis, decreased collagen deposition into the muscle, reduced apoptosis of the myofibres and reduced accumulation of damaged organelles. Furthermore, the treatment preserved the regenerating ability of muscle, assessed as an increased number of centronucleated myofibres and uniform CSA distribution. These latter results suggest in particular that LPD maintains the number and function of myogenic precursor cells. Autophagy has indeed been shown to have roles as promoter of stem cell maintenance and in a variety of cell differentiation processes, including in cellular reprogramming.[28] Our results are consistent with a similar role of autophagy also in myogenic precursor cells.

We cannot exclude that the beneficial effects of LPD treatment depend on mechanisms other than autophagy, for example, by increased muscle homoeostasis.[29] Altogether, however, our findings suggest that a proper autophagic flux contributes significantly to rescue the dystrophic phenotype and that stimulation of autophagy represents a new pharmacological strategy in DMD.

Our results contribute to explain recent findings about an amelioration of the dystrophic phenotype using the mTOR inhibitor.[30] Rapamycin, however, may not be an appropriate long-term treatment for human DMD, because it completely blocks muscle growth of regenerating myofibres[31,32] and has intrinsic toxicity. Our results explain also why enhancement of autophagy by the AMP-activated protein kinase stimulating agent 5-aminoimidazole-4-carboxamide 1-β-D-ribofuranoside, tested specifically in the diaphragm of *mdx* mice, leads to muscle functional and structural improvement.[33] Although this compound may be developed further for clinical application in DMD, the efficacy in humans of the treatment we report here can be tested immediately and safely.

Several other compounds acting on the pathways different from autophagy are now being explored in novel therapeutic strategies for DMD. Among these exon skipping and stem cell approaches appear a significant step forward to resolutive therapy, although not yet developed to a sufficient level of efficacy, as the results of the last clinical trials indicate.[2,34–36] Classical pharmacological approaches based on drugs targeting inflammation, fibrosis, epigenetic DNA modifications and redox modifications are also being tested, with favourable perspectives.[37–44] In this scenario, the therapeutic approach that we propose appears of significant value: although we do not expect an approach targeting only autophagy to be resolutive, it can be safely used in combination with cell and gene therapies and with the other drugs currently being explored for treatment of DMD. Thus, it can achieve a synergic effect and possibly lead to drug-sparing regimes. In particular, in the case of steroids, a drug-sparing regime may be of particular value limiting their adverse reactions, which appear to be severe in approximately a third of the treated patients.[45]

In conclusion, this study demonstrates the existence of a defect in autophagy in human and mouse muscular dystrophy, and that a treatment restoring autophagy ameliorates the dystrophic phenotype. Inhibition of muscle damage and inflammation, as well as maintenance of muscle regenerative capacity, appears to account for the therapeutic effect of this treatment.

Materials and Methods

Animals and treatments. C57BL/6 WT mice (C57Bl10SnJ strain) were purchased from Charles River (Wilmington, MA, USA), *mdx* mice (C57Bl10-*mdx* strain) from Jackson (Bar Harbor, ME, USA) and treated in accordance with the European Community guidelines and with the approval of the Institutional Ethical Committee.

The mice were housed in an environmentally controlled room (23 °C, 12 h light–dark cycle) and provided food and water *ad libitum*. For specific experiments, groups of mice (15 animals per group) were fed with either SD or LPD (see Table 1 for its composition). For starvation experiments, chow was removed in the morning and mice (15 animals per group) were maintained for 6 or 15 h with no food but free access to water. In the experiments with chloroquine, *mdx* mice (15 animals per group) were subjected to intraperitoneal injection with chloroquine diphosphate (50 mg/kg body weight; Sigma-Aldrich, Milano, Italy) every 24 h for 7 days.

Human muscle sample. Normal and DMD muscle samples were obtained from the 'Bank of DNA, cell lines and nerve-muscle cardiac tissue' of the Neurological Unit of the Foundation IRCCS Ca' Granda- Ospedale Maggiore Policlinico of Milan, which is part of the Telethon Genetic Biobank network of Italy.

***In vivo* functional tests.** The Whole Body Tension procedure was used to determine the ability of mice to exert tension in a forward pulling manoeuvre that is elicited by stroking the tail. The Whole Body Tension reflects the maximal acute phasic force the mouse can achieve to escape a potentially harmful event. The tails of the mice (SD or LPD-fed) were connected to a Grass FT03 transducer

(Astro-Med Industrial Park, West Warwick, RI, USA) with a 4.0 silk thread (one end of the thread being tied to the tail and the other end to the transducer). Each mouse was placed into a small tube constructed of a metal screen with a grid spacing of 2 mm. The mice entered the apparatus and exerted a small resting tension on the transducer. Forward pulling movements were elicited by a standardised stroke of the tail with serrated forceps, and the corresponding forward pulling tensions were recorded using a Grass Polyview recording system. Between 20 and 30 strokes of the tail, forward pulling tensions were generally recorded during each session. The Whole Body Tension was determined by dividing the average of the top 5 or top 10 forward pulling tensions, respectively, by the body weight.

Histology and immunohistochemistry. The animals were killed by cervical dislocation, and TA or diaphragm muscles were dissected and immediately frozen in liquid N2-cooled isopentane. For histological analyses, serial muscle sections were obtained and stained in H&E following standard procedures.[46] The number of necrotic and centronucleated fibres was counted and analysed using the public domain software MBF_ImageJ for Microscopy (http://www.macbiophotonics.ca/index.htm).

To measure CSA of individual myofibres, muscle sections were stained with an anti-Laminin A (L1293; Sigma-Aldrich) antibody. Laminin, a major component of the basal lamina, was detected using an appropriate secondary antibody, and nuclei were visualised with the DNA dye 4′,6-diamidino-2-phenylindole (DAPI). Masson's Trichrome staining was used for identifying collagen inside the muscle tissue, following standard protocols.[40]

Morphometry. Morphometric analyses were performed on sections collected from similar regions of each TA and diaphragm muscles. Two images were captured from each section and Image 1.63 (Scion Corporation, Frederick, MD, USA) was used to determine the CSA of 700–1.000 myofibres per section.[47]

EBD injection. As a measure for membrane permeability, the vital dye EBD was used. In all, 50 ml/g body weight of a 5 mg/ml solution of EBD (Sigma-Aldrich) prepared in physiological saline was injected i.v. through the tail vein. Mice were killed 18 h after EBD injection.

Apoptosis assay. Apopotsis was assessed by the TUNEL method on 10-μm cryosections using an *in situ* apoptosis detection kit (DeadEnd Fluorometric TUNEL System; Promega, Milano, Italy), according to the manufacturer's protocol. Sections were counterstained with DAPI and mounted with Vectashield (Vector Laboratories, Burlingame, CA, USA). The data were expressed as TUNEL index, calculated by counting the number of TUNEL-positive nuclei divided by the DAPI-positive nuclei. The TUNEL index was calculated from four random and non-overlapping fields.

Fluorescent and phase-contrast image acquisition and manipulation. Fluorescent and phase-contrast images were taken on microscopes (Leica DMI4000 B automated inverted microscope; lenses: HCX PL FLUOTAR $\times$10/0.30, HI PLAN I $\times$40/0.59 and HCX PL FLUOTAR $\times$100/1.30). Images were acquired using a DFC490 digital colour camera (Leica Microscopy Systems, Heerbrugg, Switzerland) and the acquisition software LAS AF (Leica Microscopy Systems). Images were assembled in panels using Photoshop 7.0 (Abobe System Software, Dublin, Ireland).

Electron microscopy. For transmission electron microscopy (TEM) analysis, entire diaphragms and TA from WT and *mdx* mice were dissected after the killing and fixed for 1 h in a solution containing 4% paraformaldehyde and 0.5% glutaraldehyde in 0.1 M cacodylate buffer, pH 7.4, immobilised on a Sylgard coated Petri dish to prevent muscular contraction. The muscles were rinsed in the same buffer and further dissected into smaller blocks (1 mm^3) that were subsequently processed for TEM as described elsewhere.[48] Briefly, the samples were postfixed with osmium tetroxide (2% in cacodylate buffer), rinsed, *en bloc* stained with 1% uranyl acetate in 20% ethanol, dehydrated and embedded in epoxy resin (Epon 812; Electron Microscopy Science, Hatfield, PA, USA) that was baked for 48 h at 67 °C. Thin sections were obtained with an ultramicrotome (Reichert Ultracut E and UC7; Leica Microsystems, Vienna, Austria), stained with uranyl acetate and lead citrate, and finally examined with a Philips CM10 TEM (FEI, Eindhoven, Germany).

Protein isolation and western blotting. Tissue samples from TA and diaphragm muscles were homogenised in a lysis buffer containing 20 mM Tris · HCl (pH 7.4), 10 mM EGTA, 150 mM NaCl, 1% Triton X-100, 10% glycerol supplemented with a cocktail of protease and phosphatase inhibitors (Sigma, St. Louis, MO, USA). Samples were centrifuged at 1.000 $\times$ *g* for 10 min at 4 °C to discard nuclei and cellular debris. Protein concentration was determined by the bicinchoninic acid assay (Pierce, Thermo Fisher Scientific, Rockford, IL, USA). Homogenates were separated by SDS-PAGE and proteins were transferred to nitrocellulose membranes (Amersham Pharmacia, Piscataway, NJ, USA). The membranes were probed using the following antibodies anti: phospho- AMPKα (Thr172) (2531), AMPKα (2532), 4E-BP1 (9644), phospho-4E-BP1 (Thr37 and Thr46) (2855), Akt (9272), phospho-Akt (Ser473) (9271), S6 (2317) and phospho-S6 (Ser240 and Ser244) (2215), all obtained from Cell Signaling Technology (Billerica, MA, USA). Antibodies to β-Actin (A5441), LC3 (L7543) and p62 (P0067) were from Sigma.

After immunostaining with the appropriate secondary horse radish peroxidase-conjugated goat anti-rabbit or anti-mouse antibodies (from Cell Signaling, Beverly, CA, USA, and Bio-Rad, Milano, Italy, respectively), bands were revealed using the Amersham ECL detection system (GE Healthcare, Fairfield, CT, USA) and quantified by densitometry using the public domain software MBF_ImageJ for Microscopy (http://www.macbiophotonics.ca/index.htm).

Real-time PCR. Tissue samples were homogenised, and RNA was extracted using the TRIzol protocol (Invitrogen, Carlsbad, CA, USA). After solubilisation in RNase-free water, first-strand cDNA was generated from 1 μg of total RNA using the ImProm-II Reverse Transcription System (Promega, Madison, WI, USA). Specific sets of primer pairs, described in Table 2, were designed to hybridise to unique regions of the appropriate gene sequence. Real-time PCR was performed using the SYBR Green Supermix (Bio-Rad) on a Roche LightCycler 480 Instrument (Roche Diagnostics, Rotkreuz, Switzerland). All reactions were run as triplicates. Samples were analysed using the Roche LightCycler 480 Software (release 1.5.0) and the second derivative maximum method. The fold increase or decrease was determined relative to a control after normalising to the internal standard 36b4.

Statistical analyses. Values were expressed as means $\pm$ S.E.M. The statistical significance of the differences between means was assessed by independent Student's *t*-test or by one-way ANOVA followed by the Bonferroni post-test to determine which groups were significantly different from the others. A probability of $<5\%$ ($P<0.05$) was considered to be significant.

Table 1 Nutritional profile of the diets used in the study

	Standard diet (SD)	Low-protein diet (LPD)
Proteins (%)	22.5	5.0
Fat (%)	5.4	10.0
Fibres (%)	3.6	4.3
Carbohydrates (%)	66.5	76.2
Minerals and vitamins (%)	2.5	4.5
Energy (kcal/g)	4.03	4.15

The diets were designed as described previously.[11]

Table 2 Primers used for quantitative real-time RT-PCR analyses

	Forward primer	Reverse primer
Atg12	5′-ATTGCTGTGGGGTTTTTCTG-3′	5′-AACCCCAGGATTTTCAGAGG-3′
Bnip3	5′-TTCCACTAGCACCTTCTGATGA-3′	5′-GAACACGCATTTACAGAACAA-3′
Gabarap	5′-CATCGTGGAGAAGGCTCCTA-3′	5′-ATACAGCTGGCCCATGGTAG-3′
LC3	5′-ACTGCTCTGTCTTGTGTAGGTT-3′	5′-TCGTTGTGTGCCTTTATTAGTGCATC-3′
36b4	5′-AGGATATGGGATTCGGTCTCTTC-3′	5′-TCATCCTGCTTAAGTGAACAAACT-3′

Conflict of Interest

The authors declare no conflict of interest.

Acknowledgements. This work was supported by the European Community's framework programme FP7/2007-2013 under grants agreements no. 241440 (ENDOSTEM) and 223098 (OPTISTEM) (to EC), the Italian Ministry of Health RC 2012 (to EC), Associazione Italiana Ricerca sul Cancro (AIRC IG11362) (to EC) and Telethon (GTB07001ER) (to MM).

1. Emery AE. The muscular dystrophies. *Lancet* 2002; **359**: 687–695.
2. Pichavant C, Aartsma-Rus A, Clemens PR, Davies KE, Dickson G, Takeda S *et al.* Current status of pharmaceutical and genetic therapeutic approaches to treat DMD. *Mol Ther* 2011; **19**: 830–840.
3. Dubowitz V. Prednisone for Duchenne muscular dystrophy. *Lancet Neurol* 2005; **4**: 264.
4. Muntoni F, Fisher I, Morgan JE, Abraham D. Steroids in Duchenne muscular dystrophy: from clinical trials to genomic research. *Neuromuscul Disord* 2002; **12**(Suppl 1): S162–S165.
5. Shintani T, Klionsky DJ. Autophagy in health and disease: a double-edged sword. *Science* 2004; **306**: 990–995.
6. Raben N, Hill V, Shea L, Takikita S, Baum R, Mizushima N *et al.* Suppression of autophagy in skeletal muscle uncovers the accumulation of ubiquitinated proteins and their potential role in muscle damage in Pompe disease. *Hum Mol Genet* 2008; **17**: 3897–3908.
7. Sandri M. Autophagy in skeletal muscle. *FEBS Lett* 2010; **584**: 1411–1416.
8. Masiero E, Agatea L, Mammucari C, Blaauw B, Loro E, Komatsu M *et al.* Autophagy is required to maintain muscle mass. *Cell Metab* 2009; **10**: 507–515.
9. Vergne I, Roberts E, Elmaoued RA, Tosch V, Delgado MA, Proikas-Cezanne T *et al.* Control of autophagy initiation by phosphoinositide 3-phosphatase Jumpy. *EMBO J* 2009; **28**: 2244–2258.
10. Risson V, Mazelin L, Roceri M, Sanchez H, Moncollin V, Corneloup C *et al.* Muscle inactivation of mTOR causes metabolic and dystrophin defects leading to severe myopathy. *J Cell Biol* 2009; **187**: 859–874.
11. Grumati P, Coletto L, Sabatelli P, Cescon M, Angelin A, Bertaggia E *et al.* Autophagy is defective in collagen VI muscular dystrophies, and its reactivation rescues myofiber degeneration. *Nat Med* 2010; **16**: 1313–1320.
12. Grumati P, Coletto L, Sandri M, Bonaldo P. Autophagy induction rescues muscular dystrophy. *Autophagy* 2011; **7**: 426–428.
13. Dogra C, Changotra H, Wergedal JE, Kumar A. Regulation of phosphatidylinositol 3-kinase (PI3K)/Akt and nuclear factor-kappa B signaling pathways in dystrophin-deficient skeletal muscle in response to mechanical stretch. *J Cell Physiol* 2006; **208**: 575–585.
14. Peter AK, Crosbie RH. Hypertrophic response of Duchenne and limb-girdle muscular dystrophies is associated with activation of Akt pathway. *Exp Cell Res* 2006; **312**: 2580–2591.
15. Mammucari C, Milan G, Romanello V, Masiero E, Rudolf R, Del Piccolo P *et al.* FoxO3 controls autophagy in skeletal muscle in vivo. *Cell Metab* 2007; **6**: 458–471.
16. Zhao J, Brault JJ, Schild A, Cao P, Sandri M, Schiaffino S *et al.* FoxO3 coordinately activates protein degradation by the autophagic/lysosomal and proteasomal pathways in atrophying muscle cells. *Cell Metab* 2007; **6**: 472–483.
17. Millay DP, Sargent MA, Osinska H, Baines CP, Barton ER, Vuagniaux G *et al.* Genetic and pharmacologic inhibition of mitochondrial-dependent necrosis attenuates muscular dystrophy. *Nat Med* 2008; **14**: 442–447.
18. Culligan K, Banville N, Dowling P, Ohlendieck K. Drastic reduction of calsequestrin-like proteins and impaired calcium binding in dystrophic mdx muscle. *J Appl Physiol* 2002; **92**: 435–445.
19. Maiuri MC, Zalckvar E, Kimchi A, Kroemer G. Self-eating and self-killing: crosstalk between autophagy and apoptosis. *Nat Rev Mol Cell Biol* 2007; **8**: 741–752.
20. Komatsu M, Waguri S, Koike M, Sou YS, Ueno T, Hara T *et al.* Homeostatic levels of p62 control cytoplasmic inclusion body formation in autophagy-deficient mice. *Cell* 2007; **131**: 1149–1163.
21. Mammucari C, Schiaffino S, Sandri M. Downstream of Akt: FoxO3 and mTOR in the regulation of autophagy in skeletal muscle. *Autophagy* 2008; **4**: 524–526.
22. Klionsky DJ, Abeliovich H, Agostinis P, Agrawal DK, Aliev G, Askew DS *et al.* Guidelines for the use and interpretation of assays for monitoring autophagy in higher eukaryotes. *Autophagy* 2008; **4**: 151–175.
23. Mizushima N, Yamamoto A, Matsui M, Yoshimori T, Ohsumi Y. *In vivo* analysis of autophagy in response to nutrient starvation using transgenic mice expressing a fluorescent autophagosome marker. *Mol Biol Cell* 2004; **15**: 1101–1111.
24. Hegge JO, Wooddell CI, Zhang G, Hagstrom JE, Braun S, Huss T *et al.* Evaluation of hydrodynamic limb vein injections in nonhuman primates. *Hum Gene Ther* 2010; **21**: 829–842.
25. Carlson CG, Makiejus RV. A noninvasive procedure to detect muscle weakness in the mdx mouse. *Muscle Nerve* 1990; **13**: 480–484.
26. Matsuda R, Nishikawa A, Tanaka H. Visualization of dystrophic muscle fibers in mdx mouse by vital staining with Evans blue: evidence of apoptosis in dystrophin-deficient muscle. *J Biochem* 1995; **118**: 959–964.
27. Sartori R, Milan G, Patron M, Mammucari C, Blaauw B, Abraham R *et al.* Smad2 and 3 transcription factors control muscle mass in adulthood. *Am J Physiol Cell Physiol* 2009; **296**: C1248–C1257.
28. Vessoni AT, Muotri AR, Okamoto OK. Autophagy in stem cell maintenance and differentiation. *Stem Cells Dev* 2012; **21**: 513–520.
29. Homsher E, Kean CJ. Skeletal muscle energetics and metabolism. *Annu Rev Physiol* 1978; **40**: 93–131.
30. Eghtesad S, Jhunjhunwala S, Little SR, Clemens PR. Rapamycin ameliorates dystrophic phenotype in mdx mouse skeletal muscle. *Mol Med* 2011; **17**: 917–924.
31. Bodine SC, Stitt TN, Gonzalez M, Kline WO, Stover GL, Bauerlein R *et al.* Akt/mTOR pathway is a crucial regulator of skeletal muscle hypertrophy and can prevent muscle atrophy in vivo. *Nat Cell Biol* 2001; **3**: 1014–1019.
32. Pallafacchina G, Calabria E, Serrano AL, Kalhovde JM, Schiaffino S. A protein kinase B-dependent and rapamycin-sensitive pathway controls skeletal muscle growth but not fiber type specification. *Proc Natl Acad Sci USA* 2002; **99**: 9213–9218.
33. Pauly M, Daussin F, Burelle Y, Li T, Godin R, Fauconnier J *et al.* AMPK activation stimulates autophagy and ameliorates muscular dystrophy in the mdx mouse diaphragm. *Am J Pathol* 2012; **181**: 583–592.
34. Goemans NM, Tulinius M, van den Akker JT, Burm BE, Ekhart PF, Heuvelmans N *et al.* Systemic administration of PRO051 in Duchenne's muscular dystrophy. *N Engl J Med* 2011; **364**: 1513–1522.
35. Bowles DE, McPhee SW, Li C, Gray SJ, Samulski JJ, Camp AS *et al.* Phase 1 gene therapy for Duchenne muscular dystrophy using a translational optimized AAV vector. *Mol Ther* 2012; **20**: 443–455.
36. Cirak S, Feng L, Anthony K, Arechavala-Gomeza V, Torelli S, Sewry C *et al.* Restoration of the dystrophin-associated glycoprotein complex after exon skipping therapy in Duchenne muscular dystrophy. *Mol Ther* 2012; **20**: 462–467.
37. Sciorati C, Miglietta D, Buono R, Pisa V, Cattaneo D, Azzoni E *et al.* A dual acting compound releasing nitric oxide (NO) and ibuprofen, NCX 320, shows significant therapeutic effects in a mouse model of muscular dystrophy. *Pharmacol Res* 2011; **64**: 210–217.
38. Minetti GC, Colussi C, Adami R, Serra C, Mozzetta C, Parente V *et al.* Functional and morphological recovery of dystrophic muscles in mice treated with deacetylase inhibitors. *Nat Med* 2006; **12**: 1147–1150.
39. Sciorati C, Buono R, Azzoni E, Casati S, Ciuffreda P, D'Angelo G *et al.* Co-administration of ibuprofen and nitric oxide is an effective experimental therapy for muscular dystrophy, with immediate applicability to humans. *Br J Pharmacol* 2010; **160**: 1550–1560.
40. Brunelli S, Sciorati C, D'Antona G, Innocenzi A, Covarello D, Galvez BG *et al.* Nitric oxide release combined with nonsteroidal antiinflammatory activity prevents muscular dystrophy pathology and enhances stem cell therapy. *Proc Natl Acad Sci USA* 2007; **104**: 264–269.
41. Fairclough RJ, Perkins KJ, Davies KE. Pharmacologically targeting the primary defect and downstream pathology in duchenne muscular dystrophy. *Curr Gene Ther* 2012; **12**: 206–244.
42. D'Angelo MG, Gandossini S, Martinelli Boneschi F, Sciorati C, Bonato S, Brighina E *et al.* Nitric oxide donor and non steroidal anti inflammatory drugs as a therapy for muscular dystrophies: evidence from a safety study with pilot efficacy measures in adult dystrophic patients. *Pharmacol Res* 2012; **65**: 472–479.
43. Colussi C, Mozzetta C, Gurtner A, Illi B, Rosati J, Straino S *et al.* HDAC2 blockade by nitric oxide and histone deacetylase inhibitors reveals a common target in Duchenne muscular dystrophy treatment. *Proc Natl Acad Sci USA* 2008; **105**: 19183–19187.
44. De Palma C, Clementi E. Nitric oxide in myogenesis and therapeutic muscle repair. *Mol Neurobiol* 2012; doi:10.1007/s12035-012-8311.
45. Manzur AY, Kuntzer T, Pike M, Swan A. Glucocorticoid corticosteroids for Duchenne muscular dystrophy. *Cochrane Database Syst Rev* 2008; CD003725; doi:10.1002/14651858.
46. Sciorati C, Galvez BG, Brunelli S, Tagliafico E, Ferrari S, Cossu G *et al. Ex vivo* treatment with nitric oxide increases mesoangioblast therapeutic efficacy in muscular dystrophy. *J Cell Sci* 2006; **119**(Part 24): 5114–5123.
47. Deponti D, Francois S, Baesso S, Sciorati C, Innocenzi A, Broccoli V *et al.* Necdin mediates skeletal muscle regeneration by promoting myoblast survival and differentiation. *J Cell Biol* 2007; **179**: 305–319.
48. Francolini M, Brunelli G, Cambianica I, Barlati S, Barbon A, La Via L *et al.* Glutamatergic reinnervation and assembly of glutamatergic synapses in adult rat skeletal muscle occurs at cholinergic endplates. *J Neuropathol Exp Neurol* 2009; **68**: 1103–1115.

Supplementary Information accompanies the paper on Cell Death and Disease website (http://www.nature.com/cddis)